

# Hydraulic fracture height limits and fault interactions in tight oil and gas formations

Samuel A. Flewelling,<sup>1</sup> Matthew P. Tymchak,<sup>1</sup> and Norm Warpinski<sup>2</sup>

Received 12 April 2013; revised 27 June 2013; accepted 28 June 2013; published 26 July 2013.

[1] The widespread use of hydraulic fracturing (HF) has raised concerns about potential upward migration of HF fluid and brine via induced fractures and faults. We developed a relationship that predicts maximum fracture height as a function of HF fluid volume. These predictions generally bound the vertical extent of microseismicity from over 12,000 HF stimulations across North America. All microseismic events were less than 600 m above well perforations, although most were much closer. Areas of shear displacement (including faults) estimated from microseismic data were comparatively small (radii on the order of 10 m or less). These findings suggest that fracture heights are limited by HF fluid volume regardless of whether the fluid interacts with faults. Direct hydraulic communication between tight formations and shallow groundwater via induced fractures and faults is not a realistic expectation based on the limitations on fracture height growth and potential fault slip. **Citation:** Flewelling, S. A., M. P. Tymchak, and N. Warpinski (2013), Hydraulic fracture height limits and fault interactions in tight oil and gas formations, *Geophys. Res. Lett.*, 40, 3602–3606, doi:10.1002/grl.50707.

## 1. Introduction

[2] Recent advancements in directional drilling and hydraulic fracturing (HF) have allowed for oil and gas extraction in tight formations (permeability  $\leq 10^{-16}$  m<sup>2</sup>). Despite the use of HF since the late 1940s [Montgomery and Smith, 2010], increased use of these techniques in the United States (U.S.) has raised concerns about potential environmental and human health effects associated with subsurface migration of HF fluid and brine. One of the main concerns is the hypothesized creation of induced fractures and shear slip along natural features (e.g., joints and faults) that might connect target formations and overlying potable aquifers. Several recent studies [Myers, 2012; Rozell and Reaven, 2012; Warner *et al.*, 2012] and the United States Environmental Protection Agency [EPA, 2012] have identified this pathway as a potential risk to potable groundwater, but none has evaluated the physical limits on hydraulic fracture growth or fault movement and how such limits might factor into an analysis of potential fluid migration to shallow aquifers.

[3] An extensive microseismic data set was presented by Fisher and Warpinski [2011], who used the shallowest and deepest microseisms as indicators of the maximum vertical extent of fracture growth (i.e., fracture heights). These data indicated that hydraulic fractures have remained far below potable groundwater in a range of U.S. sedimentary basins; however, Fisher and Warpinski did not derive bounding relationships for hydraulic fracture height growth. In this paper we present a simple physical relationship that describes the upper limit on fracture height growth as a function of HF fluid volume. We compare this limit to over 12,000 HF stimulations whose fracture networks were mapped with microseismic sensors. The observed vertical extent of microseismicity during HF stimulations in this data set is generally less than the theoretical predictions across the range of physical conditions encountered throughout the U.S. and Canada. The observed microseismic magnitudes (−4.4 to 0.86) suggest that the areas of shear displacement (including fault slip) related to HF have radii on the order of 10 m or less (assuming circular slip areas). Shear displacements along areas in this size range are unlikely to contribute significantly to either the maximum achievable fracture height or the extent of vertical fluid migration. Based on the depth range of HF stimulations and the nature of fracture growth across this range, our analysis indicates that direct hydraulic communication between tight formations and shallow groundwater is not a realistic expectation.

## 2. Derivation of Fracture Height Limit and the Observed Extent of Microseismicity

[4] A simple fracture height-limit function can be derived by considering a simple energy balance. In order to hydraulically fracture a formation, energy is needed to (1) counteract the least compressive stress ( $\sigma_3$ ; compression is positive), (2) displace the walls of the fracture, (3) propagate the fracture (i.e., crack the rock at the fracture tip), and (4) counteract energy dissipation due to fluid viscosity and leakage across the fracture face (leakoff).

[5] During HF stimulations, fluid is pumped down a well at a time-varying flow rate ( $Q$ ), which creates a time-varying pressure at the bottom of the borehole ( $P_{bh}$ ). The total energy is  $\int P_{bh} Q dt$ . Maximum possible fracture growth (i.e., tallest fractures) would occur when all energy is used to counteract  $\sigma_3$  and produce fracture width (i.e., items 1 and 2 above) in a single vertical planar fracture. Energy loss due to cracking the rock at the fracture tip is typically small for tall fractures [Engelder, 1993]; however, energy lost to the formation of complex fracture networks (e.g., multiple fractures that propagate simultaneously [Pollard and Aydin, 1988]) and fluid

<sup>1</sup>Gradient, Cambridge, Massachusetts, USA.

<sup>2</sup>Pinnacle—A Halliburton Service, Houston, Texas, USA.

Corresponding author: S. A. Flewelling, Gradient, 20 University Road, Cambridge, MA 02138, USA. (sflewelling@gradientcorp.com)

©2013. The Authors.

This is an open access article under the terms of the Creative Commons Attribution-NonCommercial-NoDerivs License, which permits use and distribution in any medium, provided the original work is properly cited, the use is non-commercial and no modifications or adaptations are made. 0094-8276/13/10.1002/grl.50707

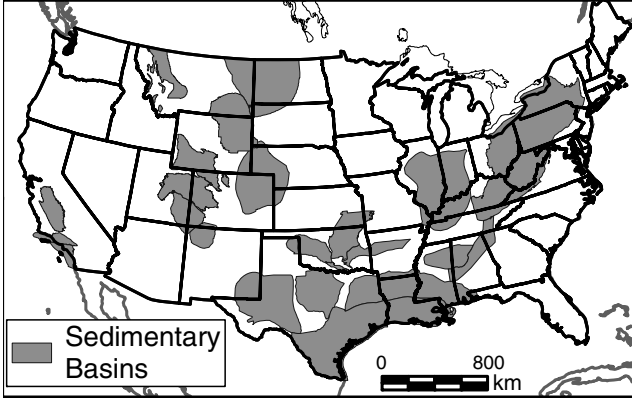


**Figure 1.** Locations of U.S. basins with microseismic data (gray regions). Note that there are also data from the Western Canadian basin (not shown).

leakoff can consume a large portion of the available energy [Nordgren, 1972]. In order to model maximum fracture heights, we represent fractures as simple planar structures with no leakoff, which approximates fracture growth in some real world cases, for example, if a fracture propagates along a preexisting joint or favorably oriented fault in low-permeability rock. Under these assumptions, the volume of HF fluid pumped into the formation is equal to the volume of the fracture created,

$$V = \frac{4}{3}\pi d \frac{HL}{2} \quad (1)$$

where  $d$  is the maximum displacement,  $H/2$  is the half height, and  $L/2$  is the half length of an ellipsoidal fracture. To simplify the analysis, we have assumed that fracture length is proportional to height,  $L = aH$ , where  $a$  is the fracture aspect ratio. Relationships for  $d$  have been reported by several authors for a linear-elastic solid of infinite aerial extent under plain-strain conditions [e.g., Pollard and Segall, 1987]. We use the following expression, which represents the maximum displacement at the center of a three-dimensional ellipsoidal fracture [Schultz and Fossen, 2002]:

$$d = \frac{2(1 - \nu^2)}{\Omega E} (P_f - \sigma_3) \frac{H}{2} \quad (2)$$

where  $\nu$  is Poisson's ratio,  $E$  is Young's modulus,  $P_f$  is fluid pressure in the fracture, and  $\Omega \cong \sqrt{1 + 1.464a^{1.65}}$  is a shape parameter [Anderson, 1995, pp. 115–116]. Similar calculations with more complicated approaches have been presented by others [e.g., Eshelby, 1957; Economides and Nolte, 2000]; however, this simple approach suffices for our bounding analysis. The difference,  $P_f - \sigma_3$ , is often referred to as the net pressure ( $P_n$ ), which we assume to be uniform throughout the fracture in this analysis. In practice,  $P_n$  may vary in the fracture with elevation above and below the midpoint. Vertical gradients in  $P_n$  may lead to various cross-sectional geometries of a fracture [Pollard, 1976]; however, for simplicity, we consider only an elliptical cross section in this analysis. Combining the above equations yields the following equation for fracture volume,

which can be rearranged to solve for fracture height (i.e., the full height of an elliptical fracture):

$$V = \frac{\pi a P_n (1 - \nu^2)}{3\Omega E} H^3, \quad (3)$$

$$H = \left[ \frac{3\Omega VE}{\pi a P_n (1 - \nu^2)} \right]^{\frac{1}{3}}. \quad (4)$$

[6] Typical ratios of  $E/P_n$  are on the order of  $10^3$  at the borehole [Fisher et al., 2002; Warpinski et al., 1990]. We take  $E$  and  $P_n$  to be effective (or average) quantities, knowing that both may vary along the fracture and differ from what is typically found at the borehole. We did not estimate aspect ratios ( $a$ ) from our microseismic data, because sensor array placement off to one side of the stimulated well creates viewing bias that may affect the accuracy of  $a$  for the microseismic cloud. Microseisms on the opposite side of the stimulated well may not be detected by the sensor array, and hence, the lateral extent of microseismicity is not characterized as accurately as the vertical extent. The upper bound fracture heights are depicted as a gray band in subsequent figures to account for a range of possible parameter combinations. The lower bound of the gray band assumes  $E/P_n = 6000$  (based on  $E = 30$  GPa and  $P_n = 5$  MPa; reasonable values at the borehole) and  $a = 1$ ; the upper bound assumes  $E/P_n = 30,000$  (to account for lower net pressure in the fracture and stiffer overlying rocks) and  $a = 0.5$ ; in both cases  $\nu = 0.2$ .

[7] We compared these maximum predicted fracture heights to measurements from microseismic monitoring of 1754 individual hydrocarbon production wells that underwent HF stimulations (both horizontal and vertical wells). Wells were located in sedimentary basins throughout the U.S. and Canada (Figure 1) and were completed in tight formations (i.e., black shale, tight sandstone, and tight carbonate). Hydraulically fractured wells may undergo a series of injections for discrete perforation intervals, known as stages. There were 12,014 individual stages for which injection volumes were recorded along with microseismic data. Approximately 57% of these data were collected in the Barnett, Eagle Ford, and Marcellus shale plays.

[8] The farthest microseisms detected above the well were used to infer the maximum potential fracture height. Wells may have microseisms both above and below the perforated segment; however, in some instances microseisms were almost entirely above the perforated segment (i.e., essentially pure upward fracture growth). Thus, the full fracture heights predicted by equation (4) are appropriate for evaluating the limit to our inferred upward fracture heights. We also note that our approach for inferring upward fracture height includes microseismicity associated with displacement near the fracture tip [Warpinski et al., 2004] and along natural features (e.g., shear displacement along preexisting joints, faults, and bedding planes). Therefore, we may overestimate upward fracture height in cases where a preexisting plane of weakness slips due to perturbation of the stress field or pore pressure beyond the fracture. A key outcome of this approach is that our fracture heights are more accurately estimates of the maximum vertical extent of seismic displacements (including slip along joints and faults).

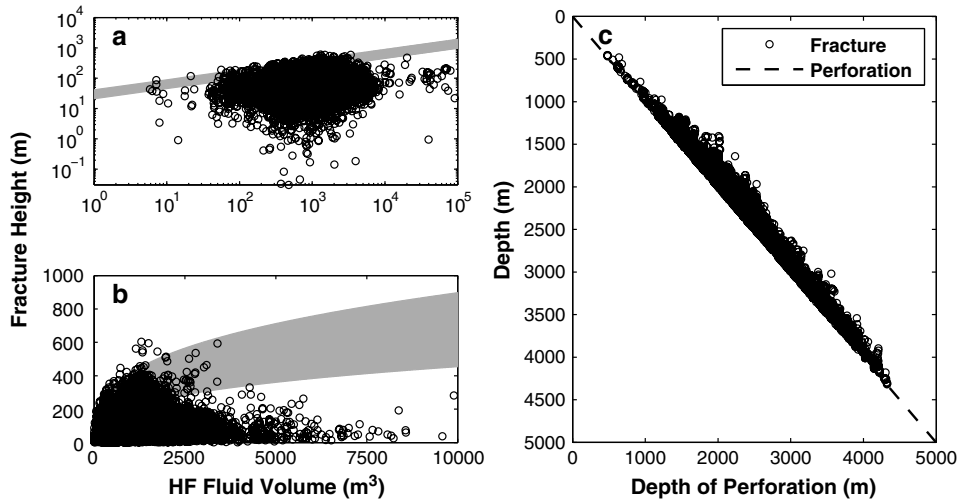


**Figure 2.** Observed upward fracture heights versus hydraulic fracture fluid volume in (a) log and (b) linear space. The gray band shows the heights predicted from equation (4), based on a range of possible parameters (see section 2). (c) The depth range of perforation midpoints and shallowest microseisms. The overburden thickness above the shallowest microseisms varies from several hundred to several thousand meters.

### 3. Observed Extent of Microseismicity Versus Theoretical Limit

[9] The observed vertical extent of microseismicity during HF stimulations was generally below the predicted uppermost limit over a range of fluid volumes that encompass 4 orders of magnitude (Figures 2a and 2b). The distribution of pumping rates ( $Q$ ) in our data set is approximately normal (mean and standard deviation in  $\text{m}^3 \text{s}^{-1}$ :  $m_Q=0.147$  and  $s_Q=0.0578$ ) and the distribution of volumes ( $V$ ) is approximately lognormal ( $\log_{10}$  mean and standard deviation in  $\text{m}^3$ :  $m_V=2.96$  and  $s_V=0.338$ ). The upper bound of the body of data lies on a straight line with a slope of 1/3 in log space (Figure 2a), consistent with equation (4) (i.e., a one-third power law). The

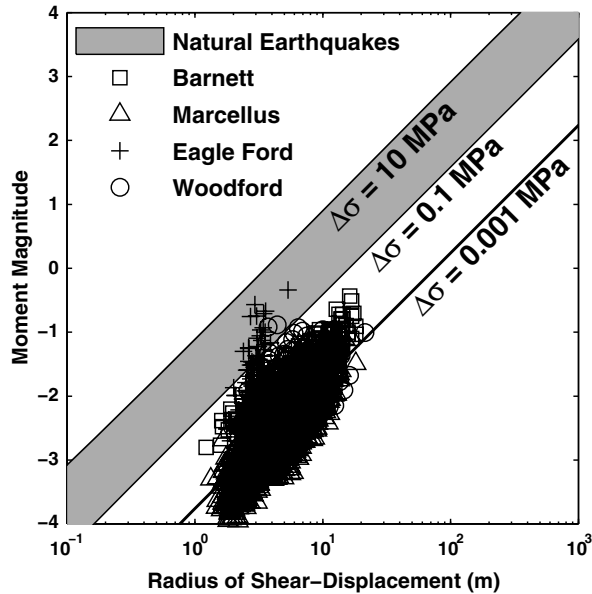


**Figure 3.** Relationship between moment magnitude and radius of shear-displacement area. The region of natural earthquakes (gray region) is based on information from Kanamori and Anderson [1975] and Zoback and Gorelick [2012].

maximum vertical extent of observed microseismicity (and hence, maximum possible fracture growth) was about 600 m. It is notable that so few data points lie above the predicted uppermost limit for reasonable parameter sets, given that the data included all detectable seismic displacements (including potential fault movements) above the well perforations.

[10] The vast majority of HF jobs in our data set were at depths >1000 m (Figure 2c). Although there are relatively few data, shallower jobs (<1000 m) exhibit a very limited extent of microseismicity above the perforated segment of the well, with only a few cases where  $H > 100 \text{ m}$ . In all of these instances, however, observed displacements remained at depths of about 500 m or greater (i.e., below the typical depth of potable groundwater). Equation (4) is likely to be valid for the deeper formations where the least principal stress is typically horizontal and fractures propagate vertically. At shallower depths, the least principal stress tends to be vertical [Brown and Hoek, 1978; Sheorey, 1994; Nadan and Engelder, 2009] and leads to horizontal rather than vertical fracture growth, as demonstrated with recent tiltmeter data [Fisher and Warpinski, 2011]. Thus, equation (4) is not appropriate at shallow depths, but fractures would not be expected to grow vertically anyway.

### 4. Fracture-Fault Interactions

[11] There are many sealed joints and faults throughout the earth’s crust, and we considered that these might be caused to slip by HF stimulations as a consequence of local stress perturbations or increased pore pressures. It is well documented that the Earth’s crust is critically stressed [Zoback, 1992; Zoback and Zoback, 1980], and brittle rocks of the upper crust (i.e., within the window of HF activities) are in a state of failure equilibrium [Zoback et al., 2002]. Therefore, injected fluids at depth can reduce normal stress and frictional resistance to slip along faults, which in turn may generate measurable seismicity. Microseismic events associated with HF are typically much smaller in magnitude ( $-4 \leq M_o \leq 0.5$ ) than felt events ( $M_o \geq 4$ ) [Dinske and Shapiro, 2013]. Nevertheless, we can use basic seismological relationships to

evaluate the areal extent of shear displacement that might be generated from HF.

[12] Seismic moments and areas of shear displacement were estimated for several of the most data-rich basins by *Warpinski et al.* [2012] and are plotted in Figure 3. For comparison, seismic moment ( $M_o = 16\Delta\sigma R^3/7$ ) was calculated for a range of static stress drops ( $\Delta\sigma$ ), assuming all seismic events were shear displacements with circular slip areas of radius,  $R$  [*Stein and Wysession, 2003*]. The data in Figure 3 indicate that the stress drops associated with the majority of HF-induced microseismicity are about 1 to 3 orders of magnitude smaller than natural earthquakes. The lower stress drops are likely associated with lower differential stress that is expected in the predominantly overpressured settings of tight oil- and gas-bearing formations [*Fischer and Guest, 2011*]. The estimated moment magnitudes are consistent with shear displacement along areas with radii on the order of 1 to 10 m. These fault length scales are consistent with the results of *Rutqvist et al.* [2013], who conducted detailed numerical simulations of HF interactions with low-permeability faults. Additionally, the vertical extent of observed microseismicity during HF stimulations is bounded by the upper vertical limit of potential fracture growth (Figure 2). This implies that the vertical extent of seismic displacements (potentially caused by perturbations in the stress field or pore pressure) is limited to the vicinity of the fracture network (i.e., the vertical extent of microseismicity is also bounded by a one-third power law). This result was previously predicted theoretically by *Shapiro et al.* [2011], who suggested that induced microseismicity during an HF stimulation should be limited to the fractured rock volume.

## 5. Implications for Potential Upward Fluid Migration

[13] Sedimentary basins are dominated by low-permeability rocks, primarily shale, siltstone, and mudstone (e.g., *Ryder et al.* [2012]; *Sandberg* [1962]), and therefore, upward fluid migration will be minimal in the absence of conductive fractures or faults. Moreover, effective vertical permeability is a harmonic mean for cross-bedding flow [*Kreitler, 1989*], meaning that the least permeable layers will control vertical permeability. Furthermore, the low water saturation in targeted formations causes any introduced water to be tightly bound by capillary forces [*Engelder, 2012*]. In this restrictive environment, the potential for upward fluid migration will depend primarily on the extent of upward fracture growth and fault movement. Our findings indicate that maximum fracture heights and the overall vertical extent of seismic displacements during HF stimulations are ultimately limited by HF fluid volume. The data in Figure 2c show that the shallowest detectable displacements in our data set occurred at about 500 m, which is below typical potable groundwater resources.

[14] The notion of upward fluid migration, as discussed in this paper, assumes that naturally occurring joints and faults are sealed and that upward fluid migration can only occur along these features when they are opened or induced to slip. Not all faults are sealed, however, and other analyses have focused on potential upward migration through open, permeable faults [e.g., *Myers, 2012*]. There is an inherent paradox regarding permeable faults and upward migration, in that hydrocarbons cannot accumulate where there are permeable

pathways for buoyant oil and gas to leak upward. Thus, the occurrence of permeable faults and significant hydrocarbon accumulations are mutually exclusive. For this reason, the issue of potential upward HF fluid and brine migration is only relevant where sealed faults are present (i.e., possible locations of hydrocarbon accumulation), and in these cases, fracture height growth and fault slip are the primary mechanisms to consider.

## 6. Conclusions

[15] Our results show that the observed vertical extent of microseismicity during HF stimulations in sedimentary basins across North America is generally constrained by a simple function of HF fluid volume. This finding suggests that maximum fracture heights and fault movements are ultimately constrained by HF fluid volume. It is not physically plausible for induced fractures to create a hydraulic connection between deep black shale and other tight formations to overlying potable aquifers, based on the limited amount of height growth at depth and the rotation of the least principal stress to the vertical direction at shallow depths. Therefore, direct hydraulic communication between tight formations and shallow groundwater via induced fractures and faults (e.g., as suggested by *Myers* [2012], *Rozell and Reaven* [2012], and *Warner et al.* [2012]) is not a realistic expectation based on the limitations on fracture height growth and potential fault slip. Other studies currently underway (e.g., the U.S. EPA National HF Study) should take into account appropriate physical constraints, such as those described here, when evaluating potential upward migration of HF fluid and brine.

[16] **Acknowledgments.** This research was funded by Halliburton Energy Services, Inc., a company that is active in the hydraulic fracturing industry in sedimentary basins around the world. The authors had sole responsibility for the writing and content of this article, and the conclusions are those of the authors. We thank Andrew Newman, Terry Engelder, and one anonymous reviewer for constructive comments that helped improve this manuscript.

[17] The editor thanks Terry Engelder and an anonymous reviewer for their assistance in evaluating this paper.

## References

- Anderson, T. L. (1995), *Fracture Mechanics: Fundamentals and Applications*, 2nd ed., CRC Press, Boca Raton, Fla.
- Brown, E. T., and E. Hoek (1978), Trends in relationships between measured in-situ stresses and depth, *Int. J. Rock Mech. Min. Sci.*, 15(4), 211–215.
- Dinske, C., and S. Shapiro (2013), Seismotectonic state of reservoirs inferred from magnitude distributions of fluid-induced seismicity, *J. Seismolog.*, 17(1), 13–25.
- Economides, M. J., and K. G. Nolte (2000), *Reservoir Stimulation*, 3rd ed., John Wiley, Chichester, U. K.
- Engelder, T. (1993), *Stress Regimes in the Lithosphere*, Princeton Univ. Press, Princeton, N. J.
- Engelder, T. (2012), Capillary tension and imbibition sequester frack fluid in Marcellus gas shale, *PNAS USA*, 109(52), E3625.
- Eshelby, J. D. (1957), The determination of the elastic field of an ellipsoidal inclusion, and related problems, *Proc. R. Soc. Lond. A Math. Phys. Sci.*, 241(1226), 376–396.
- Fischer, T., and A. Guest (2011), Shear and tensile earthquakes caused by fluid injection, *Geophys. Res. Lett.*, 38, L05307, doi:10.1029/2010GL045447.
- Fisher, K., and N. Warpinski (2011), Hydraulic fracture-height growth: Real data, SPE Annual Technical Conference and Exhibition, SPE 145949.
- Fisher, M. K., C. A. Wright, B. M. Davidson, A. K. Goodwin, E. O. Fielder, W. S. Buckler, and N. P. Steinsberger (2002), Integrating fracture mapping technologies to optimize stimulations in the Barnett Shale, SPE Annual Technical Conference and Exhibition, SPE 77441.

- Kanamori, H., and D. L. Anderson (1975), Theoretical basis of some empirical relations in seismology, *Bull. Seismol. Soc. Am.*, 65(5), 1073–1095.
- Kreitler, C. W. (1989), Hydrogeology of sedimentary basins, *J. Hydrol.*, 106(1–2), 29–53.
- Montgomery, C. T., and M. B. Smith (2010), Hydraulic fracturing: History of an enduring technology, *J. Petrol. Tech.*, 62(12), 26–32.
- Myers, T. (2012), Potential contaminant pathways from hydraulically fractured shale to aquifers, *Ground Water*, 50(6), 872–882.
- Nadan, B. J., and T. Engelder (2009), Microcracks in New England granitoids: A record of thermoelastic relaxation during exhumation of intracontinental crust, *Geol. Soc. Am. Bull.*, 121(1–2), 80–99.
- Nordgren, R. P. (1972), Propagation of a vertical hydraulic fracture, *Soc. Pet. Eng. J.*, 12(4), 306–314.
- Pollard, D. D. (1976), On the form and stability of open hydraulic fractures in the Earth's crust, *Geophys. Res. Lett.*, 3(9), 513–516.
- Pollard, D. D., and P. Segall (1987), Theoretical displacements and stresses near fractures in rock: With applications to faults, joints, veins, dikes, and solution surfaces, in *Fracture Mechanics of Rock*, edited by B. K. Atkinson, pp. 277–350, Academic Press, London.
- Pollard, D. D., and A. Aydin (1988), Progress in understanding jointing over the past century, *Geol. Soc. Am. Bull.*, 100(8), 1181–1204.
- Rozell, D. J., and S. J. Reaven (2012), Water pollution risk associated with natural gas extraction from the Marcellus Shale, *Risk Anal.*, 32(8), 1382–1393.
- Rutqvist, J., A. P. Rinaldi, F. Cappa, and G. J. Moridis (2013), Modeling of fault reactivation and induced seismicity during hydraulic fracturing of shale-gas reservoirs, *J. Pet. Sci. Eng.*, doi:10.1016/j.petrol.2013.04.023.
- Ryder, R. T., M. H. Trippi, C. S. Swezey, R. D. Crangle, R. S. Hope, E. L. Rowan, and E. E. Lentz (2012), Geologic cross-section C-C' through the Appalachian basin from Erie County, north-central Ohio, to the Valley and Ridge Province, Bedford County, south-central Pennsylvania, U. S. Geol. Surv. Scientific Investigations Map 3172.
- Sandberg, C. A. (1962), Geology of the Williston Basin, North Dakota, Montana, and South Dakota, with reference to subsurface disposal of radioactive wastes, U. S. Geol. Surv. TEI-809, 151 pp.
- Schultz, R. A., and H. Fossen (2002), Displacement–length scaling in three dimensions: The importance of aspect ratio and application to deformation bands, *J. Struct. Geol.*, 24(9), 1389–1411.
- Shapiro, S. A., O. S. Krüger, C. Dinske, and C. Langenbruch (2011), Magnitudes of induced earthquakes and geometric scales of fluid-stimulated rock volumes, *Geophysics*, 76(6), WC55–WC63.
- Sheorey, P. R. (1994), A theory for in situ stresses in isotropic and transversely isotropic rock, *Int. J. Rock Mech. Min. Sci.*, 31(1), 23–34.
- Stein, S., and M. Wysession (2003), *An Introduction to Seismology, Earthquakes and Earth Structure*, Blackwell, Malden, Mass.
- United States Environmental Protection Agency (US EPA) (2012), Study of the potential impacts of hydraulic fracturing on drinking water resources: Progress report, EPA 601/R-12/011, 278 pp.
- Wamer, N. R., R. B. Jackson, T. H. Darrah, S. G. Osborn, A. Down, K. Zhao, A. White, and A. Vengosh (2012), Geochemical evidence for possible natural migration of Marcellus Formation brine to shallow aquifers in Pennsylvania, *Proc. Natl. Acad. Sci.*, 109(30), 11,961–11,966.
- Warpinski, N. R., P. T. Branagan, A. R. Sattler, C. L. Cipolla, J. C. Lorenz, and B. J. Thorne (1990), Case study of a stimulation experiment in a fluvial, tight-sandstone gas reservoir, *SPE Prod. Eng.*, 5(4), 403–410.
- Warpinski, N. R., S. L. Wolhart, and C. A. Wright (2004), Analysis and prediction of microseismicity induced by hydraulic fracturing, *Soc. Petrol. Eng. J.*, 9(1), 24–33.
- Warpinski, N. R., J. Du, and U. Zimmer (2012), Measurements of hydraulic-fracture-induced seismicity in gas shales, *SPE Prod. Oper.*, 27(3), 240–252.
- Zoback, M. L. (1992), First- and second-order patterns of stress in the lithosphere: The World Stress Map Project, *J. Geophys. Res.*, 97(B8), 11,703–11,728.
- Zoback, M. D., and S. M. Gorelick (2012), Earthquake triggering and large-scale geologic storage of carbon dioxide, *PNAS*, 109(26), 10,164–10,168.
- Zoback, M. L., and M. Zoback (1980), State of stress in the conterminous United States, *J. Geophys. Res.*, 85(B11), 6113–6156.
- Zoback, M. D., J. Townsend, and B. Grollimund (2002), Steady-state failure equilibrium and deformation of intraplate lithosphere, *Int. Geol. Rev.*, 44(5), 383–401.